A NEW METHOD FOR THE DELAYS MEASUREMENT OF THE COMPLEX OPTICAL PULSES IN A PETAWATT CLASS LASER SYSTEMS

Mihai ȘERBANESCU[1,2], Răzvan UNGUREANU[1], Gabriel COJOCARU[1] and Paul ȘCHIOPU[2]

In this work, we present a high accuracy original method for measurement of delay between two complex optical pulses. This method was applied in an experimental case in which the delays between two signals are measured both by the derivative method and by determining the effective moments of signal generation. In this case, the measurements are free of errors generated by the amplitude of the signals and independent of the noise and parasitic reflections. These types of measurements are directly applicable in the optimization of the high power laser amplifiers, especially in the temporal synchronization of the seed and the pump pulses inside the amplifiers. For example, the high energy pump lasers are delivering double pulses per shot, temporally separated with tens of nanoseconds. The synchronization procedures of the amplifier were simplified by implementing an in-house customized delay measurement synchronization system. This paper introduces the concept and design of the control and synchronization system for the CETAL-PW laser system, as well as the experiments and results.

Keywords: delay measurements, laser amplifier, synchronization control system, complex optical pulses, dedicated software,

1. Introduction

The high power laser facilities CETAL-PW is part of INFLPR and have acquired a high power laser system (THALES, [1]) based on Chirped Pulse Amplification (CPA) technique [2] which is able to deliver high energy ultrashort pulses with optical peak power up to 1 petawatt (10^{15} W).
The laser system arrangement starts from the laser oscillator that delivers trains of individual laser pulses with few femtoseconds (1fs=10^-15 s) duration and energy of nanojoules (1nJ = 10^-9 J) with about 80 MHz repetition rate. Each of the emitted optical pulses becomes a source for electric signals as they are collected with an ultrafast photodiode. The electrical signals are used for synchronizing all the electronic devices used in this laser system. The laser pulses emitted from the

[1] Eng., Center for Advanced Laser Technologies, National Institute for Laser, Plasma and Radiation Physics, Măgurele, Romania, e-mail: mihai.serbanescu@inflpr.ro, razvan.ungureanu@inflpr.ro, gabriel.cojocaru@inflpr.ro
[2] Telecommunication and Information Technology Department, University POLITEHNICA, Bucharest, Romania, e-mail:schiopu.paul@yahoo.com

oscillator are amplified further through a multi-stage amplifier ("Front-End") up to Joule energy level. A high energy amplification stage ("PW amplifier") following the Front-End is used to amplify pulses up to 30 J.
Once the energy amplification process builds up, the repetition rate of the pulses is getting down to 0.1 Hz in the final stage.

For the optimal operation of the energetic amplification, a specific synchronization is necessary between the seed and the pumping pulses with nanosecond accuracy. In addition, it is necessary to monitor the pulse duration of the pumping lasers, usually around 15 ns.

The conceptual design of the multipass amplifier is presented in Figure 1. The main (seed) laser pulse is energetically amplified at each of the four passes through the Ti:Sa crystal. The optical path length between two passes is 6 m which corresponds to a time interval of 20 ns of light propagation, with the duration of the seed pulse of about 800 ps at half of the maximum intensity (FWHM).

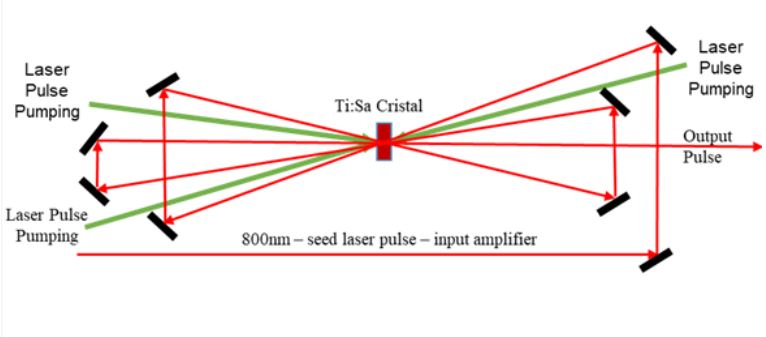

Fig.. 1. Final amplifier optical layout

To optimize the energy extraction, synchronization of the pump pulses with the seed is essential for all the passes through the gain medium [4] during an amplification event.

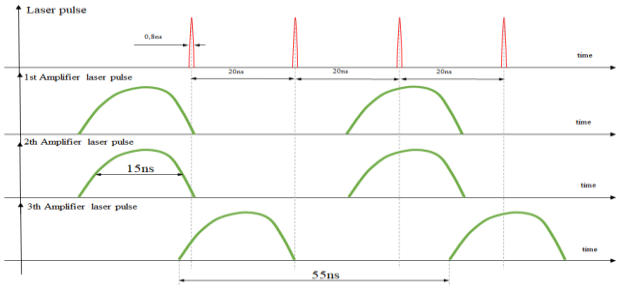

Fig. 2. Time diagram of pump and seed pulses final multipass amplifier

Each pump laser pulse has 15 ns at FWHM and provides for two pulses per shot with delays of 55 ns [5]. Correct time positioning of the pump and seed pulses

plays an important role in maximizing the gain in the amplification. The optimized diagram with the delays can be depicted in Figure 2.

2. Experimental setup

Based on the final amplifier scheme described in Fig.1 the signal measurement setup is shown in Fig. 3.

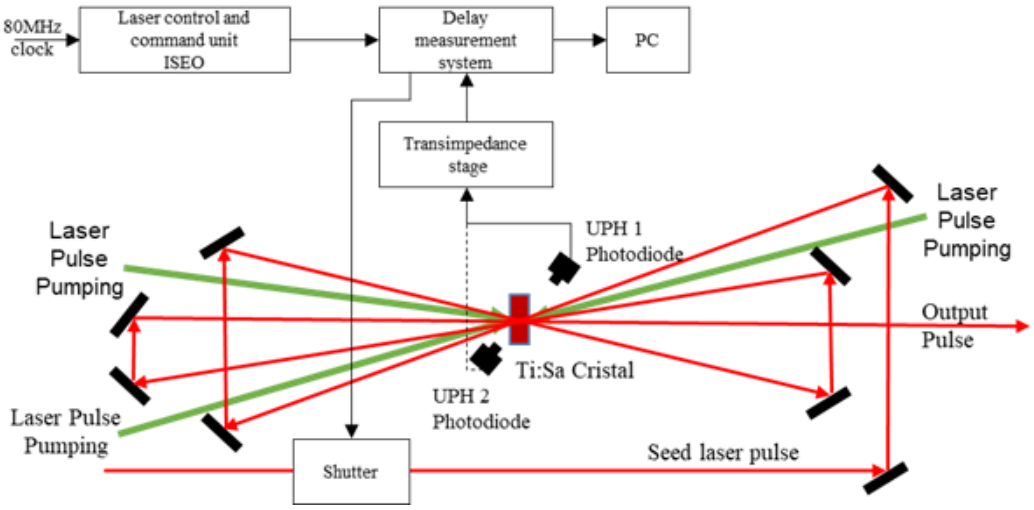

Fig.3 the experimental set-up for the signal measurements

The two fast photodiodes (UPH1, and UPH2) AlphaLas UPD-35-UVIR-D (rise time 35ps, 350nm-1700nm) alternatively measure the seed (controlled by the shutter) and the pumping pulse associated signals, then the response is transmitted to the Delay measurement system through the Transimpedance amplifier stage.

The START signal of the measurements is generated from the Laser control and command unit (ISEO) see Fig. 3.

The results measurements are displayed on the PC, which could reconfigure the control unit in the close loop.

3. Time measurement solutions

In order to optimize the amplifier operation is necessary the online monitoring of the pump pulse temporal profile, and also the delays between the pump and seed pulses.

The methods of measuring time intervals require a counter, a known and a calibrated clock signal, as well as the system of start and stop timer - START and STOP logic. The measurement resolution is given by the working frequency.

Thus, in order to measure delays at a 1 ns resolution, measurement at 50 ps time corresponding to a working frequency of 20 GHz is required.

The alternative solution is to use transfer gates with known propagation delays [6]. The time interval between the START and STOP signals is given by the number of gates through which the signal propagates. The disadvantage of the method is that the propagation time of the signal through a gate is strongly influenced by the supply voltage and temperature. The elimination of generated errors is achieved by permanent calibration by measuring a well-known time interval - the period of oscillation of a Quartz crystal. Thus, for the most unfavorable case, for variations of maximum propagation times of 50%, and for a safe measurement resolution of 66ps, an approximate measurement resolution of 44ps is required. The measured time duration is given by$T = N_P \cdot T_P$, where N_P is the number of gates through which the signal was propagated and T_p is the propagation time through a gate. In the conditions in which a clock generated by a quartz crystal with known frequency, stable with temperature, is applied at the input, its period is$T_{CK} = N_{CK} \cdot T_P$, with N_{ck} the number of gates through which the clock signal propagated. Let's consider a quartz crystal that has a known frequency and is stable with temperature and generates a clock which is applied at the input. In this case, the clock period is$T_{CK} = N_{CK} \cdot T_P$, where N_{ck} is the number of gates the clock signal propagates through. After the substitution, the measured duration is independent of the propagation time of the signal through a gate and also independent of temperature and voltage:

$$T = \frac{N_P}{N_{CK}} \cdot T_{CK} \tag{1}$$

The block diagram of a system for measuring the time between optical, generic pulses is described in Figure 3:

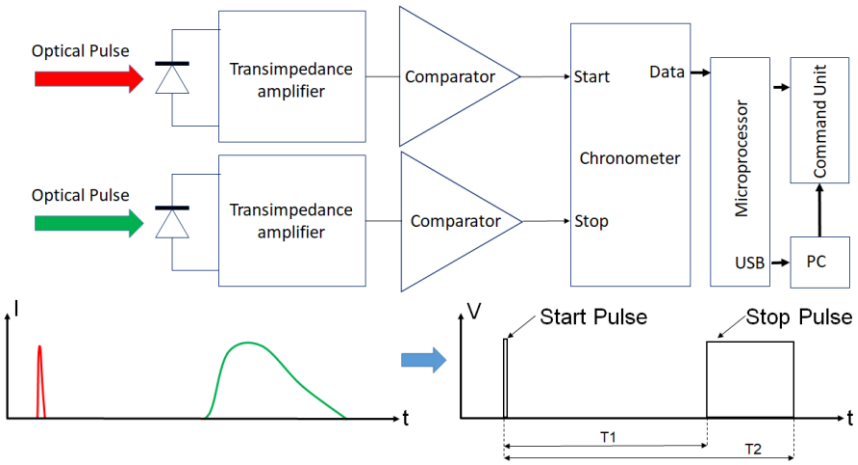

Fig. 3. Block diagram for measuring the time between optical pulses

The scheme involves the use of comparators to form digital pulses.

In the conditions in which the amplitude of the measured signals varies, measurement errors introduced by the fixed thresholds of the comparators appear [10,11], respectively shown in Fig. 4:

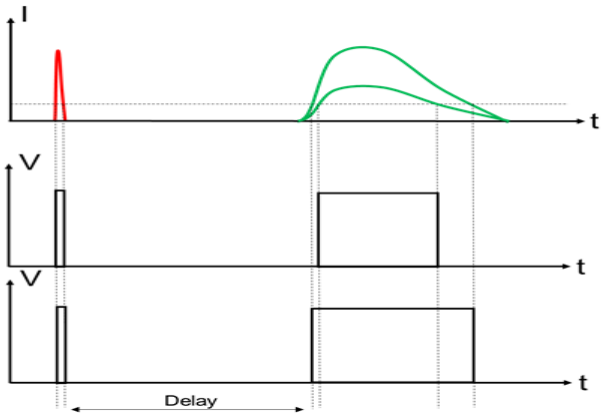

Fig. 4. Highlighting the temporal measurement errors given by the slope of the optical signals

The elimination of these errors can be done by measuring the derivatives of the input signals, respectively by measuring the time intervals between their maxima. If the output signal is contaminated with multiple reflections, the derivative will generate multiple signals, shown in Fig. 5.

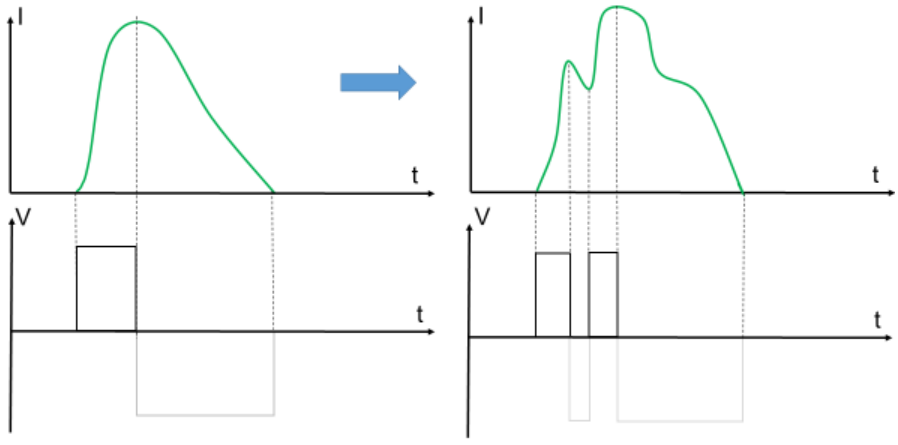

Fig. 5. Derivative of optical signals in ideal and real conditions

Therefore this method of determination cannot be applied under these conditions.

4. Time measurement system.

Within the research, a method was applied in which the delays between two signals are measured both by the derivative method and by determining the effective moments of signal generation [10, 11].

Basically, several time intervals corresponding to known levels of the tilting thresholds of the comparators in the system are measured. The actual delay is calculated according to the determined intervals, as it is shown below in Fig. 6:

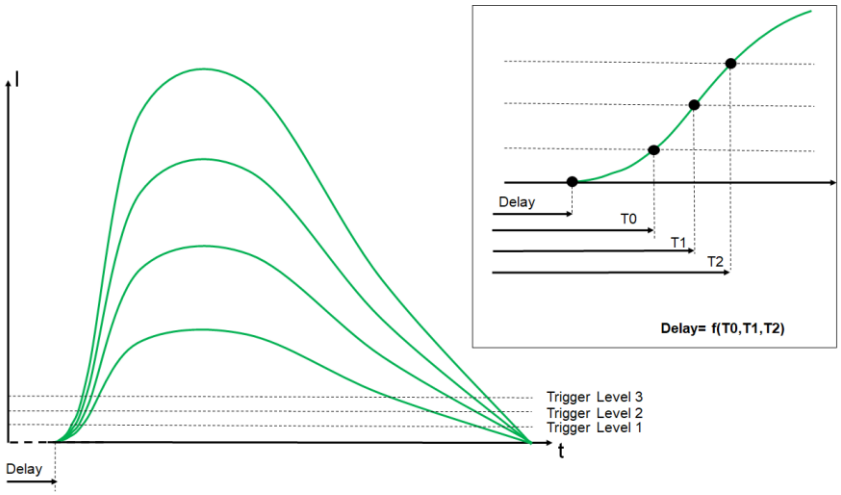

Fig.6. Determination thresholds

Basically, the times determined in the system are:

$$T_{Start} = T_{PH} + T_A + T_C$$
$$T_{StopX} = T_X + T_{PH} + T_A + T_{CX} \quad (2)$$

The times measured for the three thresholds are:

$$T_{measured\_0} = T_{Stop0} - T_{Start} = T_0 + \Delta T_{PH} + \Delta T_A + \Delta T_{C1}$$
$$T_{measured\_1} = T_{Stop1} - T_{Start} = T_1 + \Delta T_{PH} + \Delta T_A + \Delta T_{C2} \quad (3)$$
$$T_{measured\_2} = T_{Stop2} - T_{Start} = T_2 + \Delta T_{PH} + \Delta T_A + \Delta T_{C3}$$

with the delay:

$$T = f(T_0,T_1,T_2) \quad (4)$$

where:

- T is the time to be calculated;
- T_{PH} is the opening time of the photodiodes with ΔT_{PH} difference between them;

• T_A is the propagation time through the transimpedance amplifiers and ΔT_A the difference between them;
• T_C and T_{CX} are the switching times of the comparators in the system and ΔT_C the difference between them;
• ΔT and ΔT_X are the time intervals to be measured.

All times involved are dependent on temperature and supply voltage.

To eliminate these errors, a calibrated measurement is performed periodically or use the same measurement chain for alternative time delay determination in correlation with a fix Start electrical signal. Basically, the time period between the "START" signals, a digital signal generated from the laser and the optical pulse "STOP" from main laser amplifier, according to Fig. 7, are determined.

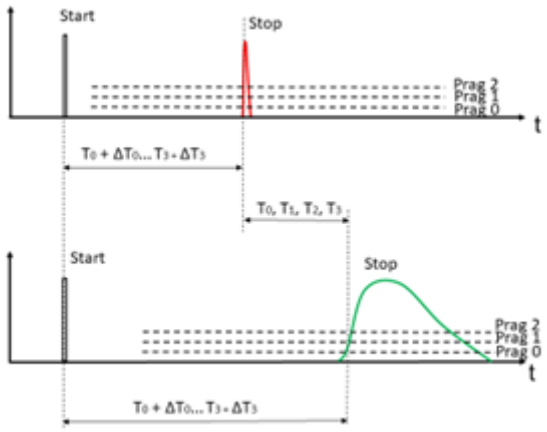

Fig. 7. Timing diagram

From the equations we obtain:

$$\begin{aligned} T_0 &= T_{measured\_0} - T_{measured\_0\_i} \\ T_1 &= T_{measured\_1} - T_{measured\_1\_i} \\ T_2 &= T_{measured\_2} - T_{measured\_2\_i} \\ T &= f(T_0,T_1,T_2) \end{aligned} \tag{5}$$

The law of composition is directly influenced by the shape of the optical beams.

In order to determine the composition law, the characteristic of the system is further determined by measuring the delays without multiple reflections, the Optical Start and Stop signals having the same shape but with different amplitudes.

The delay between the two optical signals is measured by the times between the maximums of the signals or having a comparison threshold by the half-sum of

the switching times for both the positive front (T_0) and the negative front (T_3) like in Fig. 8.

Basically the delay is:

$$T = \frac{T_0+T_3}{2} \tag{7}$$

This relationship is true only and only if $T_3 < T_0$

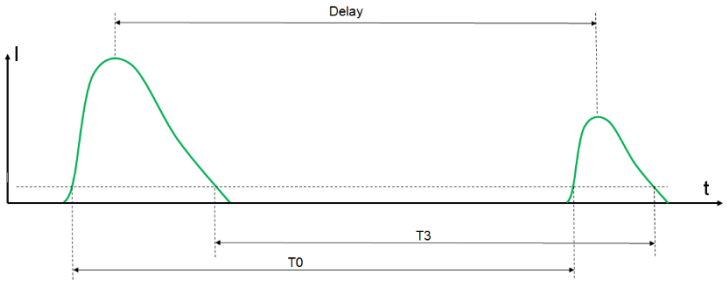

Fig. 8. Time measurement system in case of undistorted signals of multiple reflections.

Taking into account the calibrations described above the general system becomes:

$$\begin{aligned} T_0 &= T_{measured\_0} - T_{measured\_0\_i} \\ T_1 &= T_{measured\_1} - T_{measured\_1\_i} \\ T_2 &= T_{measured\_2} - T_{measured\_2\_i} \\ T_3 &= T_{measured\_3} - T_{measured\_3\_i} \\ T &= \frac{T_0 + T_3}{2} \\ T &= f(T_0,T_1,T_2) \end{aligned} \tag{8}$$

5. Implementation set-up

According to the specifications, it is necessary to use an integrated timer circuit with a measurement resolution below 50 ps and capable of measuring time intervals of 1 μs. During the implementation, we chose the integrated circuit timer type MSC Vertriebs GMBH TDC 502 [7] (45ps time resolution). This stopwatch has a start input and one or two stop inputs controlled with different slopes. Each stop input allows the recording of signals in a burst mode and can measure time intervals between successive pulses. Under these conditions, it is necessary to serialize the parallel pulses generated by the comparison thresholds, explained in Fig. 9.

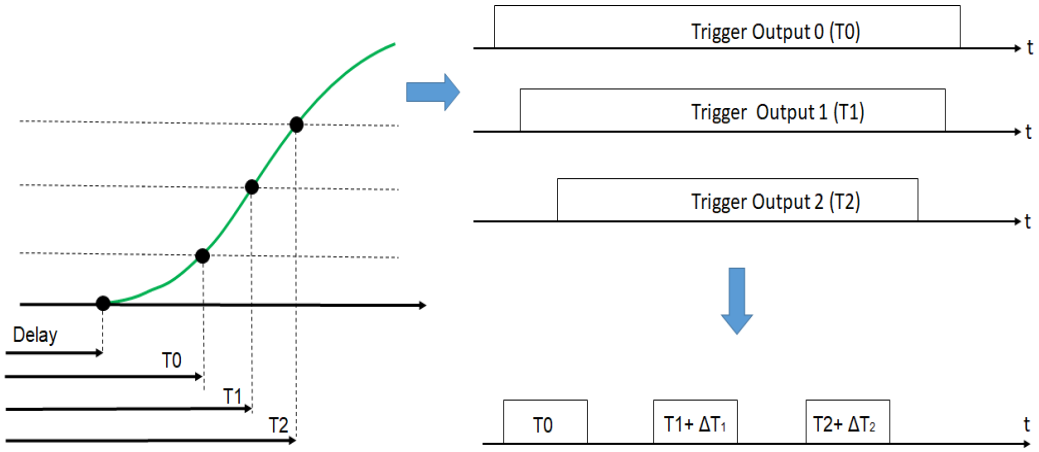

Fig. 9. Block diagram of time measurement by serialization

where:

ΔT1 and ΔT2 are the delays introduced in the system for the safe detection of pulses and were eliminated by system calibration.

Basically, four time intervals must be measured simultaneously in parallel, three for the rising front and one for the decreasing front. The usual stopwatch circuits (including the chosen circuit) allow one or two stop inputs, respectively one for ascending fronts and one for descending fronts and additionally allow cascade measurements.

The reception of the system we chose to be done with the ELECTRO-OPTIC DEVICE ERX-6 board [8] which generates two signals, one digital and one analog corresponding to the optical input of the embedded silicon photodiode. This is a compact board powered directly at 5 V and provides a transimpedance of 1000 kΩ. The central unit controls all electronic subsystems so a microcontroller must be chosen to include the necessary interfaces (CAN, Serial, parallel ports), analog-to-digital converters, counters, non-volatile and volatile memory and interrupt operation. To achieve these goals, the ATMEL AT90CAN32 microprocessor [9] was chosen, for maximum flexibility

6. Results

Statistics were performed on a series of 20-time measurements between the laser pulse and the pump laser pulse 1.

The times determined by calculation are:

- average: T = 20.2789 ns
- minimum: Tmin = 19,946 ns
- maximum: Tmax = 20,508 ns

The maximum error is: ε = ± 1.38% and the standard deviation is: σ = 0.68%. Corresponding plots are detailed in figures 10 and 11.

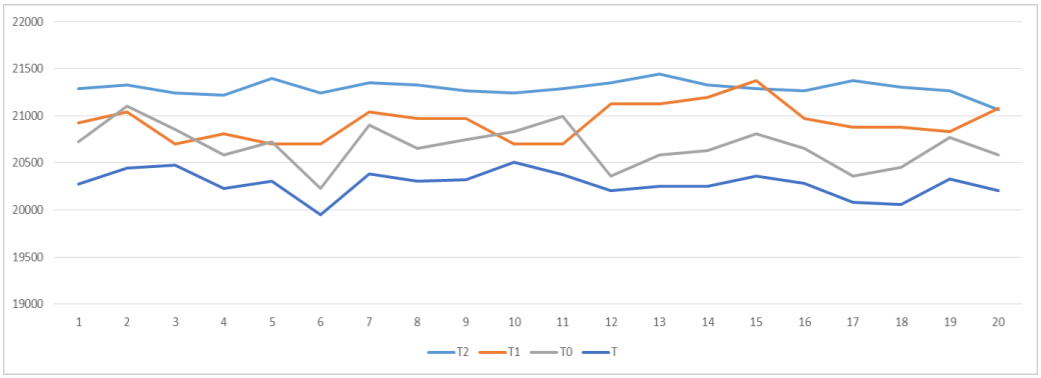

Fig. 10. Pumping time measurements 1

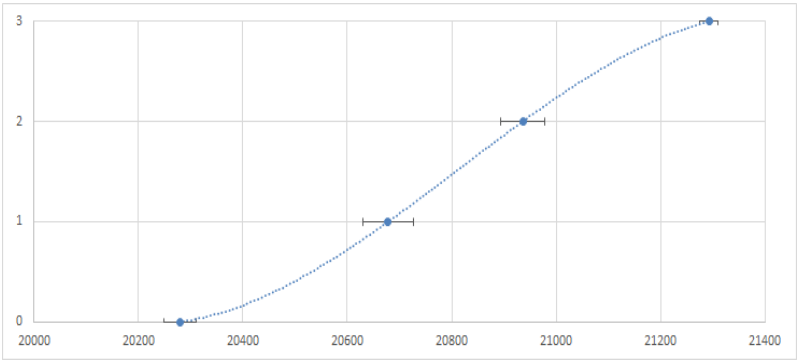

Fig. 11. Temporal points and time intervals for pump 1.

Similar statistics were performed for measurements between the laser pulse and the pump laser pulse 2 and pulse 3. For pulse 2 the results were similar to pulse 1 and for pulse 3 that are detailed in Fig. 12 and 13.

The times determined for pulse 3 by calculation are:

- average: T = 4,409 ns
- minimum: Tmin = 4,203 ns
- maximum: Tmax = 4,603 ns

The maximum error is: ε = ± 4.54% and the standard deviation is: σ = 2.31%

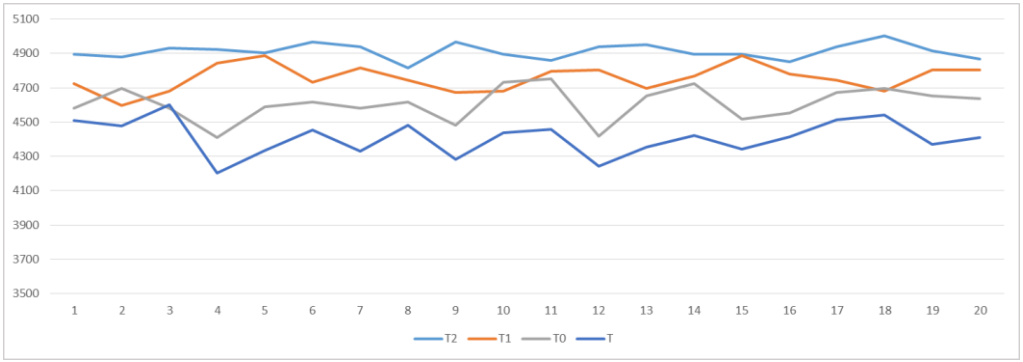

Fig. 12. Time measurements for pumping 3

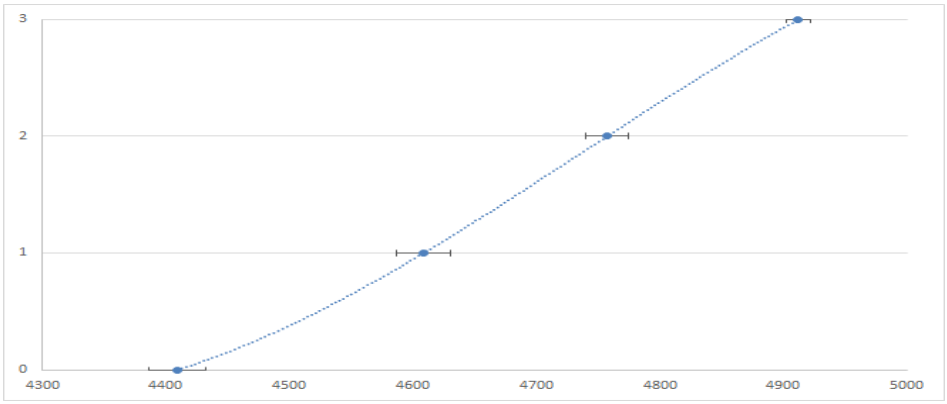

Fig. 13. Temporal points and time interval for pump 3

In the amplification of ultra-intense lasers, the synchronization between the useful pulse and the pumping pulse(s) is critical, any desynchronization generates the elimination of the optical pulse amplification or its superficial amplification. The study presented in this paper overcome this issue, in such a way that the temporal synchronization optimized the amplified laser parameters like energy, energy stability and the uniformity of the spatial beam profile.

8. Conclusions

A new method, implemented in the CETAL – PW laser system for the first time, for determining the time lags between optical pulses, with immediate application in pulse synchronization for high power laser amplifiers was presented in this paper. This new technique implements a new concept on temporal measurements between optical signals, which eliminates measurement errors due to amplitude differences between signals (slope errors) and errors generated by their parasitic multiple reflections. The temporal monitoring system ensures the determination of the phase shift between the seed pulses and the pulses of the

pumping lasers. During the implementation in the CETAL-PW laser system, the specific delays were measured, in the range of 1 ns -20 ns.

The actual research results are directly scalable to higher peak power laser facilities, such as the 2 x 10 PW ELI-NP.

Acknowledgment

This work was supported by the Romanian Ministry of Education and Research, under contract n. 8 / 2018, PN-III-P4-ID-PCCF-2016-0164, "Frontiers Research in Photon-Matter Interaction Using Extreme Helical Light Beams," acronym PMIHLB and Romanian National Nucleu Program LAPLAS VI – contract n. 16N/2019.

R E F E R E N C E S

[1]. Thales Laser, 1PW Cetal laser, https://www.thalesgroup.com/en/worldwide /group/market-specific-solutions-lasers-science-applications/lpss-lasers-science

[2] *D. Stricklan, G. Mourou*, Compression of amplified chirped optical pulses – Optics Communications, Vol. 56/3, Pag. 219-221, 1985;

[3]. *Răzvan Dabu*, „Lumina Extremă - Lasere de mare putere" Editura Academiei Române, ISBN 978-973-27-2561-0, 2015;

[4] W. Koechner, Solid State Laser Engineering, Capitolul 1, Springer Verlag,Berlin, Heidelberg, 2006

[5] Thales Laser – ATLAS25 LASER User manual, https://www.thalesgroup.com

[6] *Michael Lombardi*, The Measurement, Instrumentation, and Sensors Handbook, Edition: 2nd edition, Chapter: 41 9Time Measurement), Publisher: CRC Press, Editors: John Webster, pp.21, 2014

[7] TDC502 User Manual Version 2.6 MSC Vertriebs GmbH, https://www.mtrplus.com/en/ downloads-2/download-manuals

[8] ELECTRO-OPTIC DEVICE ERX-6, www.eodevices.com/main_erx_6_frameset.htm

[9] AT90CAN32, Microchip CPU, http://www.microchip.com/wwwproducts/en/AT90CAN32

[10]. *M. Şerbănescu, , Mihaiela Iliescu, Marian Lazar, Calin Ciufudean* - Development of 2D, Ultra-Simple, Low-Cost, Optical Range TOF Scaner laser - Latest Trends in Circuits, Systems, Signal Processing and Automatic Control, pag 91-96, ISBN: 978-960-474-374-2

[11]. *Mihaiela Iliescu, Victor Vladareanu, Mihai Serbanescu, Marian Lazar* - Sensor Input Learning for Time-of- Flight Scan Laser, "Journal of Control Engineering and Applied Informatics, vol19, No.2 pp.51-60, 2017